PCCP

Accepted Manuscript

ROYAL SOCIETY OF CHEMISTRY

www.rsc.org/pccp

Physical Chemistry Chemical Physics
CREATED USING THE RSC LaTeX PCCP ARTICLE TEMPLATE – SEE www.rsc.org/electronicfiles FOR DETAILS
ARTICLE TYPE
www. rsc.org/xxxxxx | XXXXXXXX

Towards the ionic limit of two-dimensional materials: monolayer alkaline earth and transition metal halides†

Shi-Hsin Lin,* and Jer-Lai Kuo*

We theoretically explored new two-dimensional materials near the ionic instability (three-dimensional structures are favored), with covalent bonded systems (graphene) sitting at the opposite end of the spectrum. Accordingly, monolayer alkaline earth and transition metal halides, many of their bulk forms being layered structures, were investigated with density functional calculations. We thus predicted a new class of two-dimensional materials by performing structure relaxations, cohesive/formation energies and full phonon dispersion calculations. These materials exhibit strong ionic bonding characters, as revealed by significant charge transfers. The superior charge donating/accepting abilities and the large specific area make these new materials promising for adsorption and catalytic reactions. We demonstrated adsorptions and diffusions of Li on these materials, which are relevant for Li ion battery electrodes and hydrogen storage. Also the new materials with varied charge donating abilities and their nanostructures can enhance and tune catalytic reactions, such as Ziegler-Natta catalysts. Moreover, they exhibit diverse electronic properties that can be of great application interests, ranging from insulators, metals, and even spin-polarized semiconductors.

1 Introduction

Ever since the discovery of graphene and its excellent electronic/mechanical properties [1], many research efforts were initiated on searching and investigating two-dimensional (2D) materials. The 2D nature of the material results in wider accessible areas and great strength/flexibility. The former is essential in adsorption and catalytic reactions, for instance hydrogen storage [2,3] and Li ion battery [4–6]. The latter, on the other hand, is responsible for mechanical properties. It not only implies that stable nano-structures (for instance, nanotubes, and nanoballs) can form, but also suggests possibilities to tune electronic properties by large strains that bulk materials can never sustain [7]. These advantages shared by all 2D materials make applications based on 2D materials very appealing, hence it is strongly desirable to have more 2D materials, other than graphene, to suit various purposes. For example, one with a suitable band gap would meet the needs of field effect transistors [8] or optoelectronic devices [9]. Several 2D materials have been theoretically or experimentally studied, such as hexagonal boron nitride, transition metal dichalcogenides, and many others [10–14]. More interestingly, the van der Waals heterostructures of 2D materials can be assembled in a designed manner and replenish more possibilities [15].

Among the reported 2D materials, graphene, silicene, germanene are formed with covalent bonds, boron nitride with covalent bonds as well, but with a few charge transfer between boron and nitrogen. Metal oxides or metal dichalcogenides have more charge transfer [16] due to the greater difference in electronegativities of metallic and chalcogen elements. On the other hand, for purely ionic systems, the long range Coulomb interaction favors three dimensional structures, making ionic 2D materials impossible. It is then intriguing to ask how ionic the bonds can be for 2D materials, thus providing a more complete map (Fig. 1) and understanding of 2D materials. Therefore in this work, we considered compounds composed of elements with their electronegativities close to the extremely weak or strong limits.

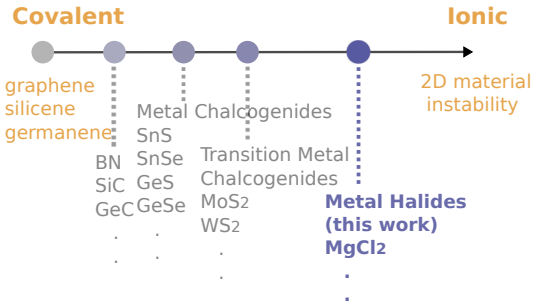

Fig. 1 Map of 2D materials. The coordinate is a rough scale of the strengths of charge transfers between the constituting elements. This work explored the 2D materials territory from the covalent bonded structures towards the ionic instability. The proposed 2D metal halides have strong ionic characters, which are promising for applications such as adsorption and catalysts.

Besides marking the border of 2D materials, the nearly

† Electronic Supplementary Information (ESI) available: [The phonon dispersions and band structures of the other 13 materials with small imaginary phonon frequencies (other than the 23 materials without imaginary phonon frequencies reported in the main text) are shown in ESI. A full list of all 36 predicted materials are summarized. Band structures calculated with the PBE functional are presented there in comparison with those calculated with LDA shown in the main text.].

* *Institute of Atomic and Molecular Sciences, Academia Sinica, No. 1, Roosevelt Rd., Sec. 4, Taipei, 10617, Taiwan. E-mail: slin2@gate.sinica.edu.tw (Shi-Hsin Lin), jlkuo@pub.iams.sinica.edu.tw (Jer-Lai Kuo)*

ionic 2D materials are very promising for applications with their ionic characters. Thin film or thin film with dispersed metals[17], and large surface area oxides, sulfides supports[18], have been extensively studied and applied in many industrial catalysts and adsorbents. Charge donating/accepting abilities and surface polarizations of materials are found crucial in many adsorption and catalytic reactions. The ionic characters of the proposed materials (composed of elements with strong electron donating/accepting abilities), together with their 2D nature (superior specific area), can potentially greatly enhance the performance of such processes.

Many 2D materials were discovered among 3D layered compounds with weakly interacting quasi-2D layers, such as graphene or MoS_2. In the mean time, crystalline structures of several halides are long known to be layered as well[19], therefore furnishing similar playgrounds to search for new 2D materials with strong ionic characters. Many of these halides are abundant in nature and have been of great application values. For example, bulk $MgCl_2$, usually extracted from brine or seawater, is utilized for dust control, ice control, hydrogen storage, and the most dominant support for the heterogeneous Ziegler-Natta catalyst in the polyolefin industry.

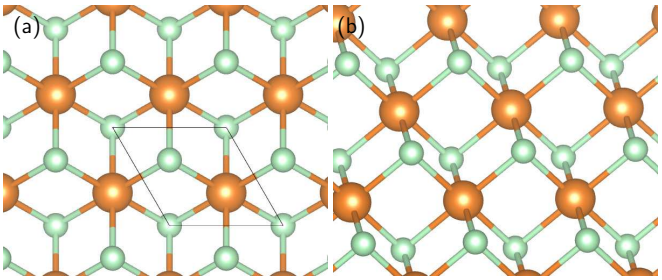

Fig. 2 Bulk $MgCl_2$ are composed of stacked layers. A $MgCl_2$ monolayer (centered honeycomb crystalline structures) is shown here: (a) top view; (b) slightly tilted top view. Orange(green) sphere represents Mg(Cl).

Therefore in this work, we began with these layered halides and adopted single layer of their centered-honeycomb lattice structures as the initial lattice structures for relaxations (For example, $MgCl_2$ in Fig. 2). Our investigations, however, are not limited to materials with their bulk forms being stacked structures since researchers nowadays were able to perform epitaxial growth of novel 2D materials on substrates. For example, silicene[20–22] and ZnO[23] 2D monolayers can be fabricated on substrates, even though the bulk Si and ZnO are not stacked layers. Thus we investigated binary compounds involving either alkaline earth metals or halogens, or both, with the the formula MX_2 (M = alkaline earth and first row transition metals; X = F, Cl, Br and I). By performing density functional calculations, we calculated 60 such binary compounds, and predicted 23 new nearly ionic 2D materials (see a more complete list of 36 materials, which include those materials with small imaginary phonon frequencies, in Electronic Supplementary Information[†]) by examining the stabilities, including structure relaxations, cohesive/formation energies and the full phonon dispersion. Possible applications for adsorption or catalytic reactions were proposed, for example hydrogen storage, Li ion battery and heterogeneous Ziegler-Natta catalysts. We also showed that these materials can exhibit a wide variety of electronic structures.

2 Method

First-principles calculations with projector-augmented-wave (PAW) potentials[24,25] were performed through the Vienna ab initio simulation package (VASP)[26,27]. Spin-polarized local density functional (LDA), generalized gradient approximation (GGA) in Perdew-Burke-Ernzerhof (PBE)[28] format and Heyd-Scuseria-Ernzerhof (HSE)[29,30] hybrid functional were adopted as the exchange correlation functionals. The plane wave cutoff energy 550 eV were used and the Brillouin zone was sampled using a $19\times19\times1$ k-point grid centered at the Γ point. A 15 Å vacuum was placed between 2D monolayers to avoid artificial interlayer couplings.

The structures were first relaxed with the conjugate gradient method, where the convergence criterion for the Hellmann-Feymann force were set to be 0.01 eV/ Å . The phonon dispersions were calculated from the dynamical matrices[31]. The required force constants were obtained by VASP density functional perturbation theory calculations with 4×4 supercells (5×5 super cells for consistent checks in some cases). Charge transfers were analyzed by the Bader analysis[32].

The calculations for adsorptions involving Li and H_2 were performed calculations using PBE functional with the dipole correction and dispersion correction using vdW-D2 method[33].

3 Result

3.1 structure and stability

We performed structure relaxations and further justified the stabilities by carrying out phonon dispersions and cohesive/formation energy calculations. The structure relaxations suggest stationary equilibrium without phonon excitations. For realistic systems, the phonons are always present. The imaginary frequencies of phonon dispersions indicate instabilities against phonon excitations, therefore the full phonon dispersions serve as a stringent criterion for structure stabilities. We found that 23 MX_2 can be stable, as shown in Fig. 3-6 with fluorides, chlorides, bromides, and iodides respectively. Aside from these 23 MX_2, for some of the investigated materials, small imaginary frequencies were found in limited regions near Γ. With a most stringent criterion, we dismissed

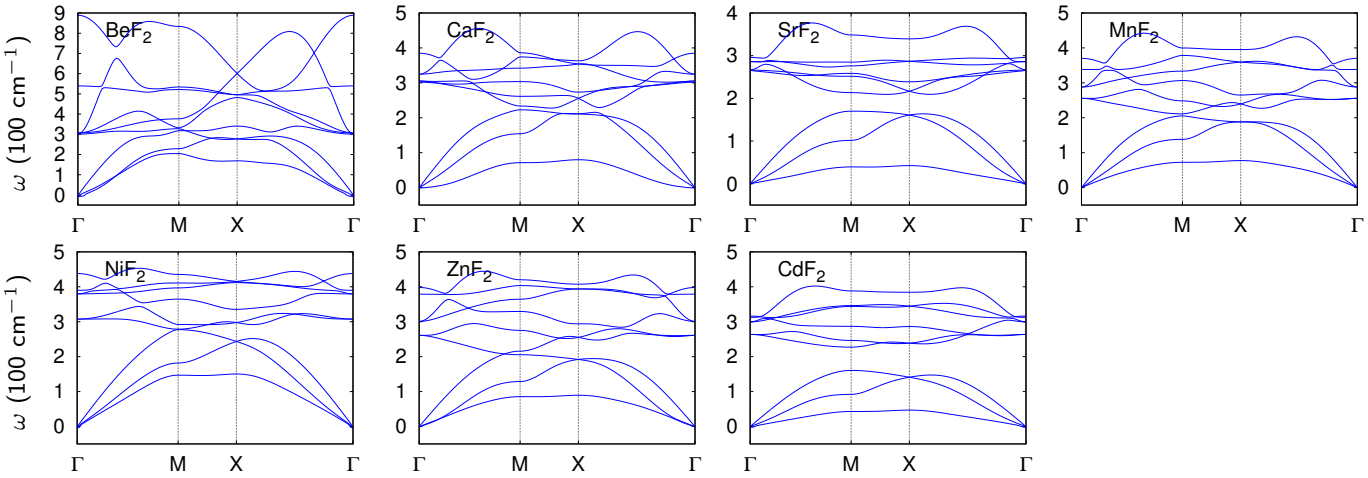

Fig. 3 Calculated phonon dispersions for fluorides.

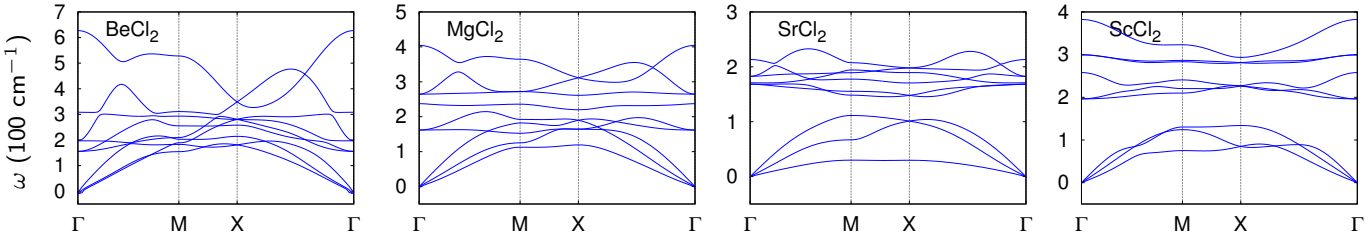

Fig. 4 Calculated phonon dispersions for chlorides.

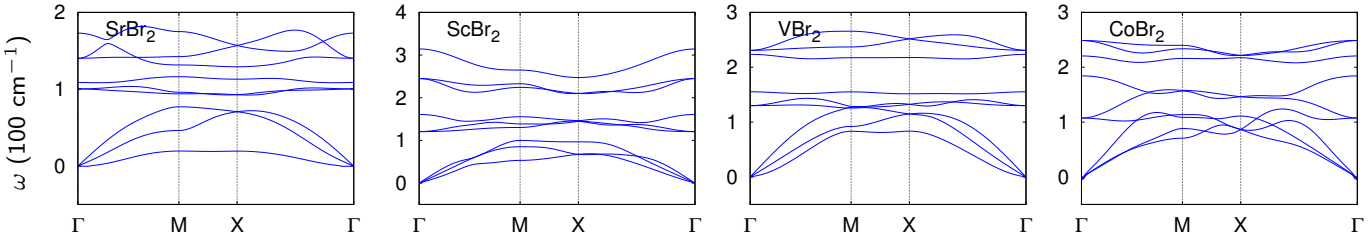

Fig. 5 Calculated phonon dispersions for bromides.

these materials in the main text and left them to the Electronic Supplementary Materials†. But it should be noted that, as discussed in details by Ataca *et al.* in Ref. 16, the phonon dispersion calculations require very high accuracy, and thus the obtained structural instability might arise from the numerical artifacts (see examples of visible imaginary frequencies for several predicted materials in Ref. 16). Many of such materials with small imaginary phonon frequencies have layered bulk structures and their monolayers possess considerable cohesive/formation energies (cf. Ref. 16 and the Electronic Supplementary Materials†).

We further attested the stabilities with cohesive and formation energies. Cohesive energy is defined as the energy benefit per unit cell relative to free constituent atoms, while formation energy relative to constituent elements in their equilibrium phases (bulk metals for all metallic elements; gas for F, Cl, and Br; solid for I)[16]. The candidates for new 2D compounds and their structural properties, cohesive/formation energies, and charge transfers between metals and halogens using LDA functional are summarized in Table 1 (see the full table including those materials with small imaginary phonon frequencies in Electronic Supplementary Materials†). Some PBE and HSE results are also shown. For those compounds that survive the phonon excitations (or with imaginary frequencies in a small region), the cohesive/formation energies are all found to be positive, except VBr_2 and FeI_2 with marginal negative forma-

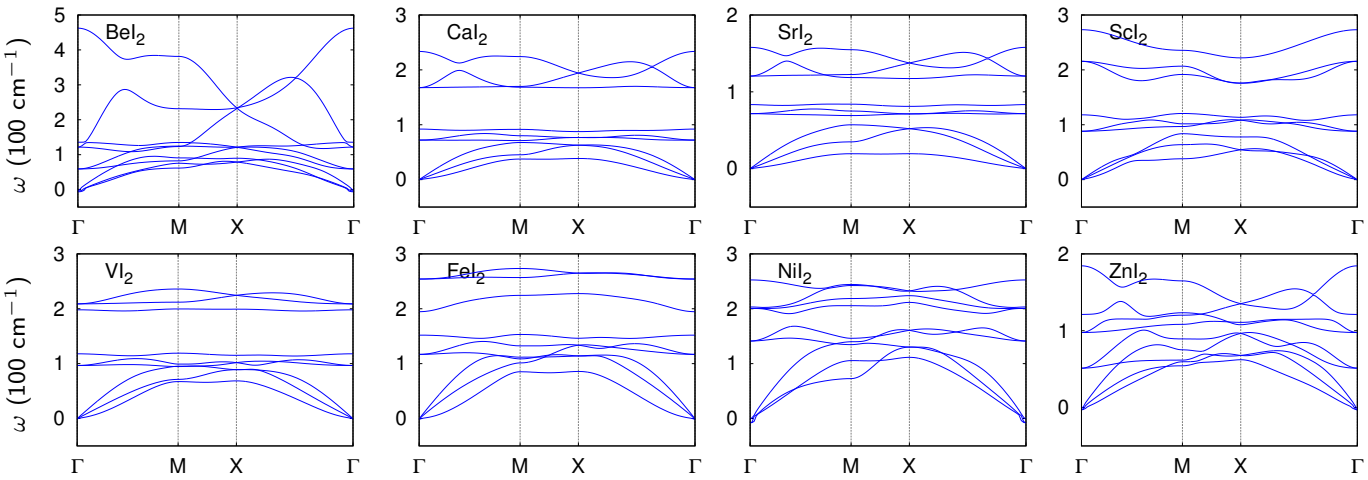

Fig. 6 Calculated phonon dispersions for iodides.

tion energies under HSE or PBE.

Volume and ionic positions relaxations using HSE functional were performed for those materials with layered bulk. The lattice constant obtained by HSE is close to that of PBE, with the difference in the order of 0.01Å. We therefore used PBE lattice constants for HSE calculations, and only relaxed the ionic positions to obtain the HSE formation energies shown in Table 1 (the error in energies are in the order of meV for those tested materials), since full HSE relaxations are quite computationally expensive. In general, the stabilities concluded from formation energies are consistent with LDA and PBE result. The lattice constants obtained by PBE are all greater than LDA as expected. The X-M-X bond angles of fluoride are smaller than other halides. This is likely due to the much smaller ionic radius of fluorine, and can also be observed in transition-metal oxides and dichalcogenides [16], where X-M-X angles of oxides are in general smaller than chalcogenides.

For those materials with layered bulk counterparts, we calculated the formation energies of their bulk counterparts to compare with that of the 2D structures. PBE with dispersion correction (vdW-D2) was adopted to properly deal with the interlayer interaction. It is found that, as shown in Table 2, most of the monolayer materials (except FeI_2) are slightly more stable than the bulk counterparts, with the formation energy differences in the range of several tens to hundreds of meV. Energies of the bulk counterparts shown here were calculated using experimental lattices. Relaxed lattices were also used, and energies of the bulk phases were lowered by several tens of meV, which does not alter the conclusion that monolayers are more stable. These materials can thus be of immediate experimental relevance utilizing the well-developed cleavage techniques.

3.2 ionic character and its implication

The charge transfers of compounds involving simultaneously alkaline earth metals and halogens are significantly greater than all currently known 2D materials, including graphene, boron nitride, transition metal oxides and dichalcogenides. For example, the charge transfer from the alkaline earth metal to the halogen for SrF_2 is $0.82e^-$, for CaF_2 is $0.79e^-$, for BeF_2 is $0.75e^-$, rendering strong ionic bonding characters. These materials thus mark the border of 2D materials since the pure ionic bonding prefers 3D structures, owing to the long range Coulomb interaction.

The ionic character of those alkaline earth metal halides is attributed to the weak (strong) electronegativities of the constituent alkaline earth metals (halogens). For those late transition metal iodides, the differences of the electronegativities of the constituent atoms are considerably smaller. Iodine has weaker electronegativity than fluorine and bromine, while late transition metals, such as Fe, Co, Ni have stronger electronegativities than other first row transition metals. Minor, or even reversed, charge transfer were observed for $CoBr_2$, FeI_2, NiI_2, and ZnI_2 (cf. Table 1). As spin-orbit coupling is strong for heavy elements, we further carried out calculations with spin-orbit coupling. The resulting charge acquired by iodine is $0.27e^-$ for $CoBr_2$, $0.34e^-$ for FeI_2, $0.24e^-$ for NiI_2, and $0.40e^-$ for ZnI_2.

These constituent elements with weak or strong electronegativities result in strong electron donating or accepting abilities, making such materials very active for adsorption and catalytic reactions. Depending on which elements (metals or halogens) are exposed, these materials exhibit different chemical activity (charge donating or accepting). For instance on the (0 0 1) plane, where halogens are exposed and the metals are sandwiched between halogens, the surface halogens can

	a (Å)		d_{M-X} (Å)	d_{X-X} (Å)	θ (deg)	E_c (eV)		E_f (eV)		ρ_M (e)	ρ_X (e)	
		PBE						PBE	HSE			
BeF_2	2.56	2.62	1.72	2.31	84.19	17.59	9.75	8.77	5.82	-1.53	0.75	×
CaF_2	3.53	3.62	2.24	2.75	75.83	17.99	12.17	11.39	11.82	-1.53	0.79	×
SrF_2	3.81	3.92	2.39	2.89	74.28	17.51	11.88	11.29	11.71	-1.64	0.82	×
MnF_2	3.24	3.35	2.10	2.65	78.56	15.40	6.51	6.95	4.90	-1.39	0.69	×
NiF_2	3.00	3.11	1.98	2.58	81.40	14.92	4.98	4.97	7.26	-1.26	0.63	×
ZnF_2	3.09	3.19	2.02	2.62	80.51	12.84	7.24	6.70	7.24	-1.35	0.68	×
CdF_2	3.46	3.57	2.22	2.79	77.69	11.89	6.62	6.34	3.28	-1.36	0.67	×
$BeCl_2$	3.17	3.26	2.21	3.07	88.09	12.02	7.06	6.70	7.06	-1.05	0.52	×
$MgCl_2$	3.56	3.67	2.47	3.42	87.68	11.55	8.90	8.85	11.26	-0.98	0.49	◯
$SrCl_2$	4.31	4.45	2.84	3.71	81.43	13.26	10.52	10.60	13.05	-1.24	0.60	×
$ScCl_2$	3.45	3.58	2.52	3.67	93.59	15.20	9.21	8.97	11.27	-1.02	0.51	-
$SrBr_2$	4.44	4.61	3.00	4.02	84.27	12.05	7.13	6.68	7.10	-1.06	0.50	×
$ScBr_2$	3.62	3.76	2.67	3.92	94.55	13.87	5.71	4.97	5.23	-0.99	0.50	-
VBr_2	3.71	3.84	2.56	3.54	87.33	12.61	2.86	2.84	-0.49	-0.63	0.32	-
$CoBr_2$	3.49	3.75	2.40	3.31	86.98	11.18	1.60	1.23	3.38	-0.05	0.03	◯
BeI_2	3.75	3.85	2.63	3.69	89.07	8.95	1.20	0.97	1.20	-0.12	0.06	-
CaI_2	4.35	4.54	3.06	4.32	89.56	10.82	5.10	5.02	5.47	-0.65	0.31	◯
SrI_2	4.63	4.84	3.22	4.46	87.87	10.65	5.12	5.26	5.74	-0.84	0.40	×
ScI_2	3.90	4.05	2.87	4.23	94.64	12.40	3.63	3.52	3.87	-0.68	0.34	-
VI_2	3.97	4.12	2.75	3.82	87.82	11.37	1.00	1.56	3.54	-0.51	0.25	-
FeI_2	3.74	3.86	2.55	3.45	85.30	10.40	0.19	-0.07	0.43	0.11	-0.06	◯
NiI_2	3.78	3.96	2.64	3.67	88.36	10.08	0.24	0.48	1.94	0.30	-0.15	◯
ZnI_2	3.95	4.10	2.78	3.93	89.69	6.92	1.42	1.52	1.88	0.00	0.00	◯

Table 1 The candidates for new 2D compounds and their structural properties, cohesive/formation energies, and charge transfers between metals and halogens using LDA functional. Some PBE and HSE results are also shown. $d_{M(X)-X}$ is the distance between M(X) and X, and θ is the X-M-X bond angle. $E_c(E_f)$ are cohesive(formation) energies defined in the text. Acquired charge of halogens(metals) without spin-orbit coupling, in unit of electron charge e^-, is $\rho_X(\rho_M)$. A ◯ (×) is used to indicate if its layered bulk counterpart can (cannot) be found in literatures. The charge transfers of compounds involving simultaneously alkaline earth metals and halogens are significant, rendering strong ionic characters.

	expt. bulk[34] a (Å)	LDA/PBE 2D a (Å)	dE (eV)
$MgCl_2$	3.60	3.56 / 3.67	-0.07
$CoBr_2$	3.68	3.49 / 3.75	-0.76
CaI_2	4.48	4.35 / 4.54	-0.47
FeI_2	4.04	3.74 / 3.86	0.18
NiI_2	3.89	3.78 / 3.96	-0.60
ZnI_2	4.25	3.95 / 4.10	-0.22

Table 2 Energy difference $dE \equiv E_{2D} - E_{bulk}$ per formula between the predicted 2D materials and their bulk counterparts, calculated by PBE functional with dispersion correction.

grab electrons from adatoms. The adatoms need to compete to lose electrons with the sandwiched metals, according to their electronegativities. The metals then serve as charge reservoirs, which can modify the charge acquiring ability of the surface halogens and hence the chemical activities or adsorptions. On the other hand, for the edges of the 2D planes, for example (1 1 0) or (1 0 0), the unsaturated metals are exposed and thus display strong charge donating abilities. We discussed possible applications, adsorptions and catalysts, of these two cases in the following.

Adsorptions are one of the important applications of 2D materials. For example, graphene decorated with metals is proposed as a strong candidate for high capacity electrodes of Li ion batteries[4–6] and hydrogen storage. In this respect, the 2D materials proposed in this work possess even more superior advantages due to the charge donating/accepting abilities. Here we discuss the possibilities for Li ion batteriese and hydrogen storag as examples. 2×2 supercell models of NiF_2 and NiI_2 sheets were used for demonstrations. We performed calculations using PBE functional with dipole and dispersion corrections using vdW-D2 method[33]. For (0 0 1) surface, halogens are exposed such that NiF_2 and NiI_2 have strong tendencies to take away electrons from Li. The adsorption energy of Li on the Ni top is found to be 3.76 eV/Li and 2.80 eV/Li for NiF_2 and NiI_2 respectively. These adsorption energies are considerably higher than the bulk Li cohesive energy 1.63 eV/atom and hence much alleviate the clustering problem that is suffered for many electrode materials of Li ion battery[35]. Comparing to graphene, the adsorption energy for graphene with a 2×2 supercell model using LDA is only around 0.8 eV[3]. The adsorption is also found to be superior to transition metal dichalcogenide MoS_2[36]. The charge transfer from Li to the substrate is significant, largely attributed to the exposed halogens, making Li greatly positively charged ($+0.906e^-$ for NiF_2 and $0.873e^-$ for NiI_2). The Coulomb repulsion between these highly positively charged Li again suppresses the Li clustering. Since positively charged Li is only attached to the surface via electrostatic forces, rather than covalent bonds, Li diffuses relatively easily on the surface, which is crucial for applications on Li ion battery electrodes. We thus calculated the diffusion barriers with the climbing image nudged elastic band (cNEB) method[37] as shown in Fig. 7(a). The diffusion barrier for Li on the metallic 2D NiI_2 from Ni top to the dented I site (see Fig. 2(b)) is 0.36 eV, comparable to that on graphene[6]. On the other hand, the highly charged Li can lead to strong adsorption of hydrogen molecules. For example, we found that one hydrogen molecule can be adsorbed on a Li decorated 2D NiF_2 (see Fig. 7(b)) with the adsorption energy 0.320 eV for a 2×2 supercell model. The adsorption energy of one hydrogen molecule on Li decorated graphene is 0.05 eV[3] using LDA. Therefore this new class of 2D materials offers a viable candidate for hydrogen storage. The hydrogen storage capability of pristine NiF_2 was also investigated. Besides Ni is less positively charged ($+0.63e^-$ as seen from Table 1), the adsorption of hydrogen molecules is further sabotaged by the three neighboring protruding negatively charged F. The resulting adsorption energy 0.048 eV is much weaker than that of the Li decorated NiF_2.

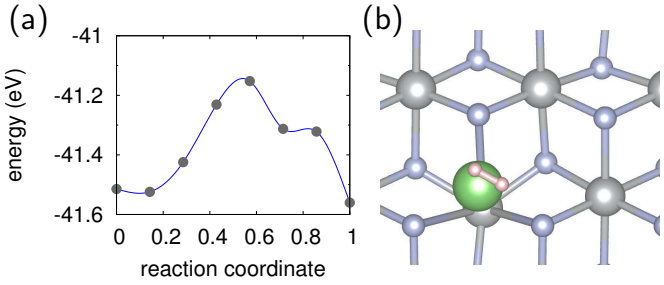

Fig. 7 (a) Lithium diffusion on the metallic 2D NiI_2 from Ni top to the dented I site. The diffusion barrier is 0.36 eV, which is suitable for Li ion battery applications. (b) Calculated geometry for one hydrogen molecule adsorbed on 2D NiF_2 sheet. The strong Li binding energy (3.76 eV/atom) on the sheet and highly positive charge ($+0.906e^-$) of Li suppress the Li clustering. The adsorption energy of hydrogen obtained by PBE with dispersion correction is 0.320 eV/H_2, significantly greater than that of graphene.

When the unsaturated alkaline earth metals are exposed on the sides of the 2D materials, the resulting strong charge donating abilities makes these class of materials ideal for the catalysts. The situation resembles the bulk $MgCl_2$ supported Ziegler-Natta catalyst, where Mg is exposed on (1 0 0) or (1 1 0) surfaces. It is shown that significant charge is donated from Mg to Ti species, leading to enhanced back donation into propylene. Charge transfers, involving $MgCl_2$ supports or added donors, are considered as an important factor in Ziegler-Natta catalysts[38–40]. In this work, the found new alkaline earth metal halides, some of which do not have layered bulk structures, can very well suit the same purpose. These materials vary in charge donating abilities, so that the properties of the corresponding final products can likely be tuned. Futhermore, the nanostructures of these materials, such as nano-ribbons, arrays, or heterostructures, supply yet another form, which can be designed to maximize the more effective planes, for instance (1 1 0) for $MgCl_2$ support. The new materials and new forms can greatly enhance or tune the catalytic reactions.

3.3 electronic structure

The band structures of the predicted 2D materials exhibit a wide breadth of electronic properties. The band gaps were extracted from calculated band structures with LDA, as shown in Fig. 8-11 and PBE, and summarized in Table 3 (band

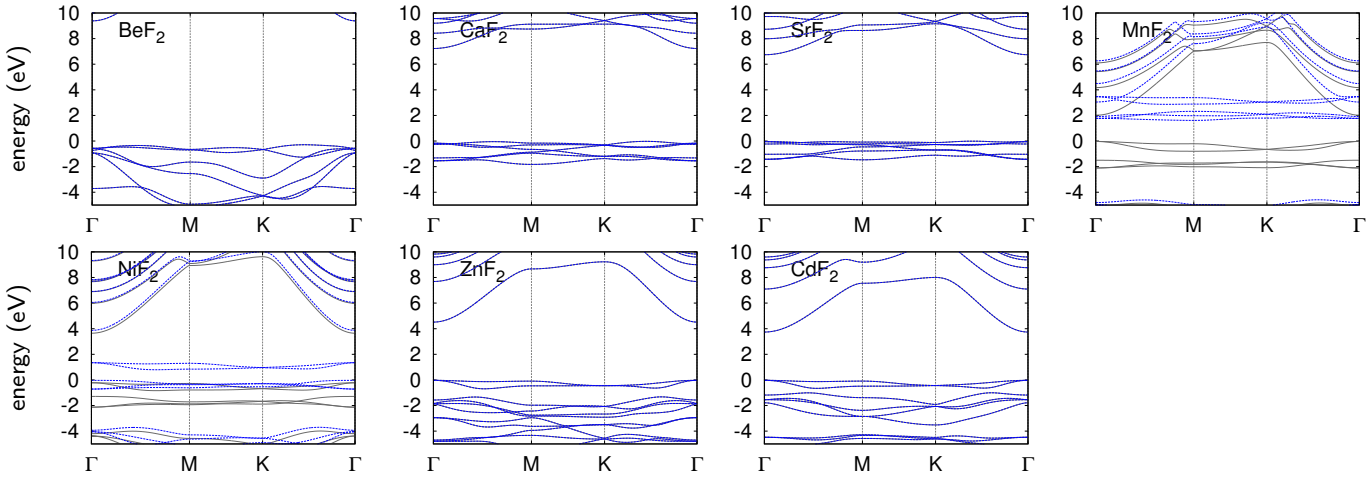

Fig. 8 Calculated band structures (LDA) for fluorides. The grey solid and blue dotted lines correspond to the two spin states.

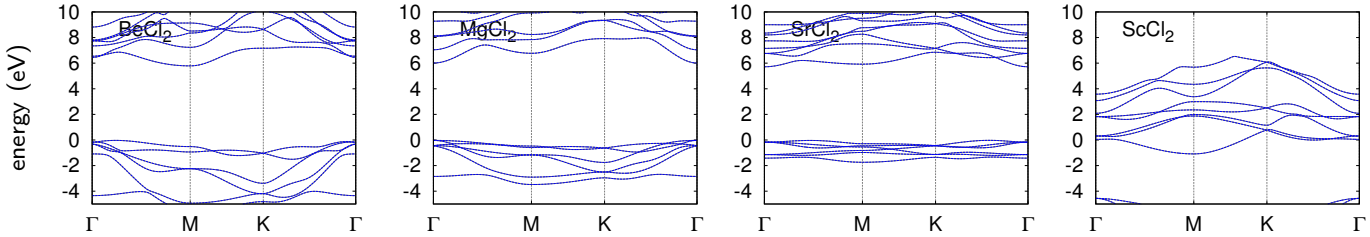

Fig. 9 Calculated band structures (LDA) for chlorides. The grey solid and blue dotted lines correspond to the two spin states.

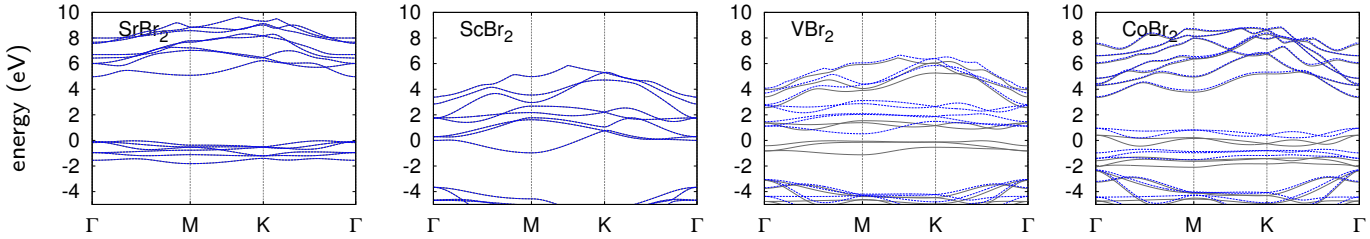

Fig. 10 Calculated band structures (LDA) for bromides. The grey solid and blue dotted lines correspond to the two spin states.

structures of those compounds with small imaginary phonon frequencies, band structures calculated with the PBE functional and a full table are shown in Electronic Supplementary Materials[†]). As LDA and PBE are usually questionable in obtaining accurate band gaps, we further performed HSE hybrid functional calculations for those metallic compounds, cf. Table 3 and Fig. 12. It should be noted, however, as noted by several researchers, that for 2D MoS_2 and several other single-layer honeycomb structures [16,41,42], band gaps predicted by LDA or PBE results agrees better with experimental values than higher level calculations such as GW. Those nearly ionic compounds, mostly alkaline earth metal halides, are salts and characterized by large band gaps in the order of 4-10 eV. These halides, being excellent 2D insulators, can be placed as insulating layers in a van der Waals heterostructure [15] of 2D materials to control the spacings between conducting planes.

Meanwhile, the transition metal halides are more versatile in their electronic properties, ranging from insulators, metals, and even spin-polarized semiconductors. Zn and Cd halides are characterized with relatively larger band gaps. Early and middle transition metal, such as Sc, V, Cr, and Mn, halides generally possess small or no band gaps. Those transition halides without band gaps can be candidates for Li ion battery as discussed in the previous section. In the meantime, the charge carriers of V, Cr, Mn, Ni, and Co halides are spin-polarized, and these halides are magnetic. Some of them have

	E_g (eV)			μ (μ_B)		
	LDA	PBE	HSE	LDA	PBE	HSE
BeF_2	9.67^i	9.25^i		0.00	0.00	0.00
CaF_2	7.25^i	7.03^i		0.00	0.03	0.01
SrF_2	6.75^i	6.49^i		0.00	0.03	0.02
MnF_2	2.05^d	2.34^d		5.00	5.00	1.00
NiF_2	0.83^i	0.99^i		2.00	2.00	2.00
ZnF_2	4.55^i	4.46^d		0.00	0.00	0.01
CdF_2	3.77^d	3.82^d		0.00	0.00	0.00
$BeCl_2$	5.82^i	5.89^i		0.00	0.00	0.00
$MgCl_2$	6.04^d	5.98^i		0.00	0.00	0.00
$SrCl_2$	5.75^i	5.75^i		0.00	0.00	0.02
$ScCl_2$	M	M	M	0.00	0.00	0.26
$SrBr_2$	5.00^i	5.01^i		0.00	0.00	0.02
$ScBr_2$	M	M	M	0.00	0.00	0.22
VBr_2	0.84^i	1.08^i		3.00	3.00	3.00
$CoBr_2$	M	0.13^i	5.54^d	1.00	3.00	3.00
BeI_2	2.41^i	2.51^i		0.00	0.00	0.00
CaI_2	3.53^i	3.91^i		0.00	0.00	0.00
SrI_2	3.95^i	4.33^i		0.00	0.00	0.01
ScI_2	M	M	M	0.00	0.00	1.00
VI_2	0.83^i	1.05^i		3.00	3.00	3.00
FeI_2	0.76^i	0.78^i		0.00	0.00	0.00
NiI_2	M	2.77^i	4.06^i	1.73	2.00	2.00
ZnI_2	1.86^i	2.03^i		0.00	0.00	0.00

Table 3 Band gaps, and magnetic moments μ_B per unit cell. The superscripts $i(d)$ of band gap values indicate indirect(direct) gaps. Metals are denoted as "M". Transition metal halides exhibit versatile electronic properties.

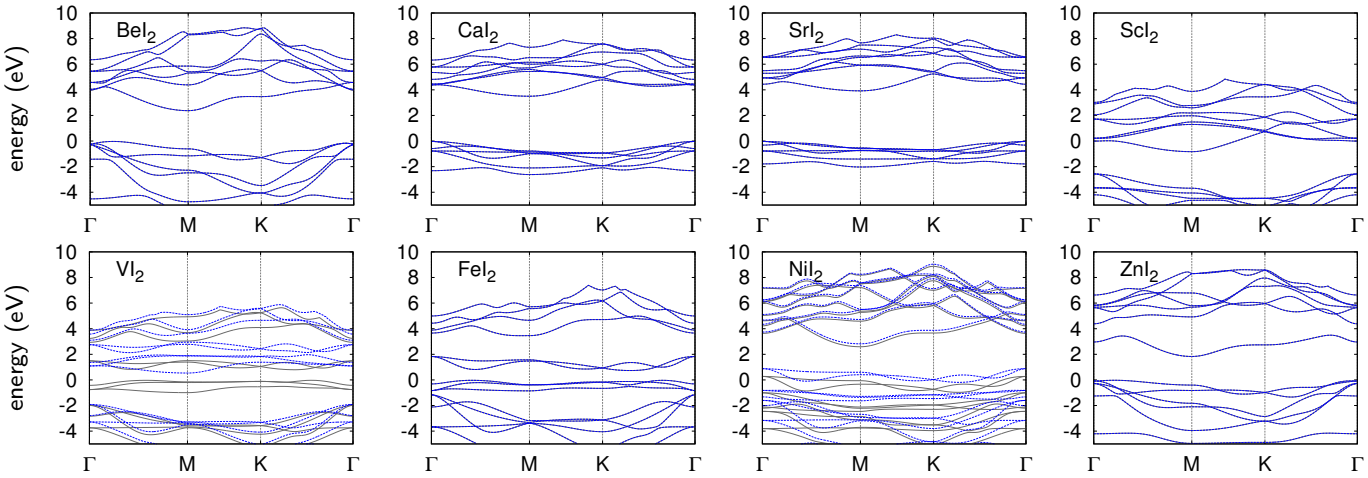

Fig. 11 Calculated band structures (LDA) for iodides. The grey solid and blue dotted lines correspond to the two spin states.

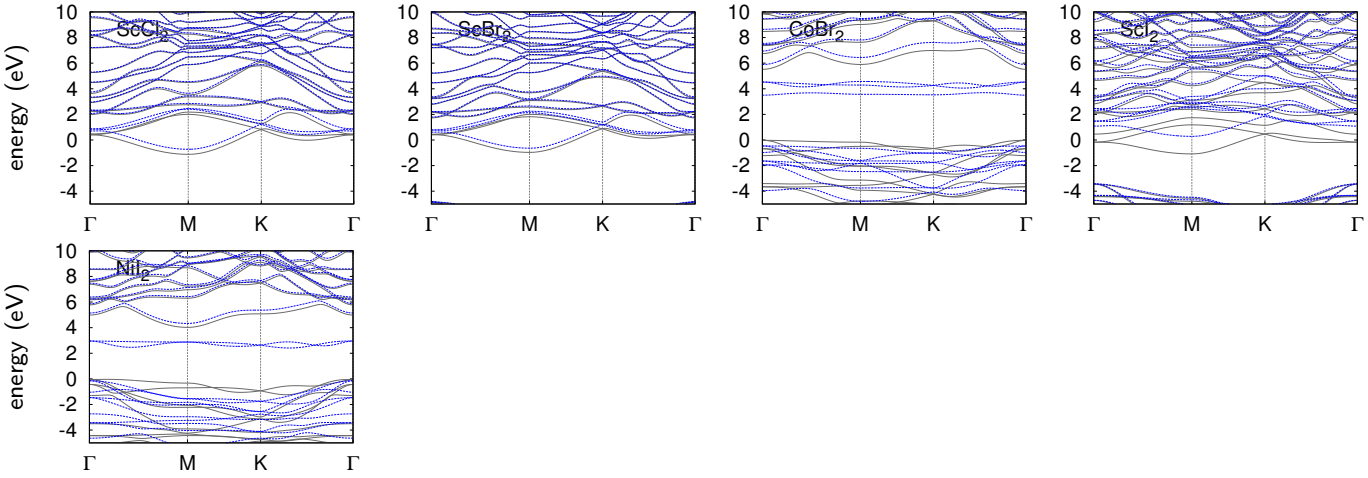

Fig. 12 Calculated band structures (HSE) for $CoBr_2$ and NiI_2. The grey solid and blue dotted lines correspond to the two spin states.

suitable band gaps for optoelectronic devices although most of the gaps are indirect. Among them, MnF_2 is a direct wide band gap semiconductor with a gap 2.05 eV, which can be utilized for optoelectronics applications. In general, band gaps decrease as d_{M-X}'s increase when X goes from F to I for MX_2. It was found that band gaps obtained by HSE are usually greater than PBE and LDA. In particular, the conduction bands of $CoBr_2$ and NiI_2 using HSE are greatly lifted compared to LDA and PBE, making them insulators, rather than metals identified by LDA or PBE. In the meantime, considerable spin polarization are found using HSE for $ScCl_2$, $ScBr_2$, and ScI_2, but absent using LDA or PBE.

4 Conclusion

In summary, we explored the ionic limit of 2D materials, and predicted new materials, based on structure relaxations, cohesive energies and full phonon dispersion calculations. Our findings provide a more complete map and understandings of 2D materials. It was found that the charge transfers of compounds involving simultaneously alkaline earth metals and halogens are significantly greater than all currently known 2D materials, including graphene, boron nitride, transition metal oxides and dichalcogenides. For example, the charge transfer from the alkaline earth metal to the halogen for SrF_2 is $0.82e^-$, for CaF_2 is $0.79e^-$, for BeF_2 is $0.75e^-$, rendering strong ionic bonding characters. The superior charge donating/accepting abilities along with the large specific area of these 2D materials enable enhancement and tunabilities of adsorption and cat-

alytic reactions. For example, the alkaline earth metal halides can be used as catalysts, for example as supports of Ziegler-Natta catalysts. The various charge donating abilities can be utilized to modify and tune the properties of final products. Their nanostructures (clusters, arrays, or heterostructures) can be designed to maximize the effective planes to promote the performance of catalysts. We also demonstrated the notable potential for electrodes of Li ion batteries or hydrogen storage with NiF_2 and NiI_2 as examples. Our calculations for a 2×2 supercell model show that adsorption energy of Li around 3.76 eV for NiF_2 and 2.80 eV for NiI_2 (considerably beyond the bulk Li cohesive energy) with highly positively charged Li ($+0.906e^-$ for NiF_2 and $+0.873e^-$ for NiI_2), suggesting suppression of Li clustering. Li diffusion barrier on NiI_2 was found to be low (0.36 eV), making it a potential new material for Li ion battery electrodes. Meanwhile, the adsorption energy of hydrogen molecules was found around 0.320 eV, significantly greater than that for graphene. Moreover, transition metal halides exhibit diverse electronic properties that can be of great application interests, ranging from insulators, metals, and even spin-polarized semiconductors. Therefore our investigations not only make impacts on fundamental physics by exploring the ionic limit of 2D materials, but also on applications of adsorptions, catalysts, and electronics.

Acknowledgments

This work was financially supported by the Academia Sinica and the National Science Council (NSC101-2113-M-001-023-MY3) of Taiwan, and the National Center for Theoretical Sciences (South) Physics Division. Computational resources are supported in part by the National Center for High Performance Computing.

References

1 A. H. Castro Neto, F. Guinea, N. M. R. Peres, K. S. Novoselov and A. K. Geim, *Rev. Mod. Phys.*, 2009, **81**, 109–162.
2 M. Zhou, Y. Lu, C. Zhang and Y. P. Feng, *Appl. Phys. Lett.*, 2010, **97**, 103109.
3 C. Ataca, E. Aktürk, S. Ciraci and H. Ustunel, *Appl. Phys. Lett.*, 2008, **93**, 043123.
4 E. Yoo, J. Kim, E. Hosono, H.-s. Zhou, T. Kudo and I. Honma, *Nano Letters*, 2008, **8**, 2277–2282.
5 X. Fan, W. Zheng and J.-L. Kuo, *ACS Appl. Mater. Interfaces*, 2012, **4**, 2432–2438.
6 X. Fan, W. T. Zheng, J.-L. Kuo and D. J. Singh, *ACS Appl. Mater. Interfaces*, 2013, **5**, 7793–7797.
7 V. M. Pereira and A. H. Castro Neto, *Phys. Rev. Lett.*, 2009, **103**, 046801.
8 B. Radisavljevic, A. Radenovic, J. Brivio, V. Giacometti and A. Kis, *Nat. Nanotechnol.*, 2011, **6**, 147–150.
9 K. F. Mak, C. Lee, J. Hone, J. Shan and T. F. Heinz, *Phys. Rev. Lett.*, 2010, **105**, 136805.
10 M. Xu, T. Liang, M. Shi and H. Chen, *Chem. Rev.*, 2013, **113**, 3766–3798.
11 R. Mas-Balleste, C. Gomez-Navarro, J. Gomez-Herrero and F. Zamora, *Nanoscale*, 2011, **3**, 20–30.
12 M. Osada and T. Sasaki, *Adv Mater*, 2012, **24**, 210–228.
13 Q. H. Wang, K. Kalantar-Zadeh, A. Kis, J. N. Coleman and M. S. Strano, *Nat. Nanotechnol.*, 2012, **7**, 699–712.
14 S. Z. Butler, S. M. Hollen, L. Cao, Y. Cui, J. A. Gupta, H. R. Gutierrez, T. F. Heinz, S. S. Hong, J. Huang, A. F. Ismach, E. Johnston-Halperin, M. Kuno, V. V. Plashnitsa, R. D. Robinson, R. S. Ruoff, S. Salahuddin, J. Shan, L. Shi, M. G. Spencer, M. Terrones, W. Windl and J. E. Goldberger, *ACS Nano*, 2013, **7**, 2898–2926.
15 A. K. Geim and I. V. Grigorieva, *Nature*, 2013, **499**, 419–425.
16 C. Ataca, H. Şahin and S. Ciraci, *J. Phys. Chem. C*, 2012, **116**, 8983–8999.
17 M. Ichikawa, in *Supported Clusters, Structure, Reactivity and Microscopic Processes in Catalysis*, ed. R. M. Lambert and G. Pacchioni, Springer, 1997, vol. 331, pp. 153–192.
18 D. Rainer and D. Goodman, *J. Mol. Catal. A: Chem.*, 1998, **131**, 259 – 283.
19 L. Pauling, *Proc. Natl. Acad. Sci. U.S.A.*, 1929, **15**, 709–712.
20 P. Vogt, P. De Padova, C. Quaresima, J. Avila, E. Frantzeskakis, M. C. Asensio, A. Resta, B. Ealet and G. Le Lay, *Phys. Rev. Lett.*, 2012, **108**, 155501.
21 A. Fleurence, R. Friedlein, T. Ozaki, H. Kawai, Y. Wang and Y. Yamada-Takamura, *Phys. Rev. Lett.*, 2012, **108**, 245501.
22 L. Meng, Y. Wang, L. Zhang, S. Du, R. Wu, L. Li, Y. Zhang, G. Li, H. Zhou, W. A. Hofer and H.-J. Gao, *Nano Letters*, 2013, **13**, 685–690.
23 C. Tusche, H. L. Meyerheim and J. Kirschner, *Phys. Rev. Lett.*, 2007, **99**, 026102.
24 P. E. Blöchl, *Phys. Rev. B*, 1994, **50**, 17953–17979.
25 G. Kresse and D. Joubert, *Phys. Rev. B*, 1999, **59**, 1758–1775.
26 G. Kresse and J. Hafner, *Phys. Rev. B*, 1993, **48**, 13115–13118.
27 F. Fuchs, J. Furthmüller, F. Bechstedt, M. Shishkin and G. Kresse, *Phys. Rev. B*, 2007, **76**, 115109.
28 J. P. Perdew, K. Burke and M. Ernzerhof, *Phys. Rev. Lett.*, 1996, **77**, 3865–3868.
29 J. Heyd, G. E. Scuseria and M. Ernzerhof, *The Journal of Chemical Physics*, 2003, **118**, 8207–8215.
30 J. Heyd, G. E. Scuseria and M. Ernzerhof, *The Journal of Chemical Physics*, 2006, **124**, –.
31 A. Togo, F. Oba and I. Tanaka, *Phys. Rev. B*, 2008, **78**, 134106.
32 G. Henkelman, A. Arnaldsson and H. Jónsson, *Comput. Mater. Sci.*, 2006, **36**, 354 – 360.
33 S. Grimme, *J. Comput. Chem.*, 2006, **27**, 1787–1799.
34 R. Wyckoff, *Crystal Structures*, Wiley, 1963.
35 J. Tarascon and M. Armand, *Nature*, 2001, **414**, 359–367.
36 H. J. Chen, J. Huang, X. L. Lei, M. S. Wu, G. Liu, C. Y. Ouyang and B. Xu, *Int. J. Electrochem. Sci.*, 2013, **8**, 2196 – 2203.
37 G. Henkelman, B. Uberuaga and H. Jonsson, *J. Chem. Phys.*, 2000, **113**, 9901–9904.
38 K. Soga and T. Shiono, *Prog. Polym. Sci.*, 1997, **22**, 1503 – 1546.
39 X. Zhao, Y. Zhang, Y. Song and G. Wei, *Surf. Rev. Lett.*, 2007, **14**, 951–955.
40 T. Taniike and M. Terano, *J. Catal.*, 2012, **293**, 39 – 50.
41 C.-H. Chang, X. Fan, S.-H. Lin and J.-L. Kuo, *Phys. Rev. B*, 2013, **88**, 195420.
42 H. Shi, H. Pan, Y.-W. Zhang and B. I. Yakobson, *Phys. Rev. B*, 2013, **87**, 155304.